Adsorption in Bidisperse-Pore Systems

Eugene E. Petersen
Dept. of Chemical Engineering, University of California, Berkeley, CA 94720

Adsorption of a strongly bound absorbate in a bidisperse-pore system is modeled using a Turner pore structure. This idealized system leads to an analytical solution for the micropore uptake of adsorption that is valid for a part of the adsorption-time profile. The analytical solution yields a well-defined criterion that establishes the boundary between an adsorption process dominated by macropore resistance and one dominated by micropore resistance. The range of the analytical solution is extended to include the entire adsorption-time profile using an approximate analytical solution and two asymptotic solutions.

Introduction

Solids with bidispersed-pore systems find applications in a wide variety of processes. Ion exchange, heterogeneous catalysis, and pressure swing adsorption are examples. The rates at which these processes take place depend on the rate of transport by diffusion in the pore network of the adsorbent. In porous media, the diffusion process itself is complicated because of our inability to characterize the geometry of the pores. The qualitative behavior of a bidisperse system depends on the relative rates of penetration of the micropores and the macropores. If the micropores are slowly penetrated compared to the macropores, the adsorbate will penetrate to the center of the macropore before appreciable penetration of the micropores has taken place. Such a system, in the limit, has the micropores bathed in an adsorbent concentration approximately the same as the outside of the pellet and adsorption rates are nearly uniform throughout the pellet. Conversely, if diffusion in the micropores is much faster than in the macropores, an adsorbate front progresses from the outside of the pellet to the center. The time for adsorbate penetration of the macropore is accordingly much longer than in the absence of the micropores. These ideas are well-known and have been discussed in the literature (Barrer, 1963; McBain, 1952).

Ruckenstein et al. (1971) modeled a spherical pellet containing microspheres in a matrix and assumed that the adsorption isotherm was linear throughout the adsorption process. The model was solved exactly, but the resulting equations were complex to use and interpret. Garg and Ruthven (1974) investigated the effects of nonlinearities in the adsorption-desorption isotherm on the pressure-swing process. More recently, Doong and Yang (1987) simplified the equation of material balance by assuming parabolic concentration profiles within the micropores.

The analysis below is based on a model of Turner (1958) shown in Figure 1. There are several reasons for selecting this model. The geometry of the macropores and the diffusivity within are well-defined. This is also true for the micropore, except that the diffusivity is not well-characterized when the adsorbate and pore diameters approach the same order of magnitude. The model is conceptually simple and the various geometric parameters are easy to visualize. Lastly, the simple geometry leads to a closed form solution over a portion of the adsorption process for the case of an adsorbate that is strongly adsorbed. "Strongly adsorbed" in this case refers to an adsorbate that essentially reaches saturation locally at low concentrations.

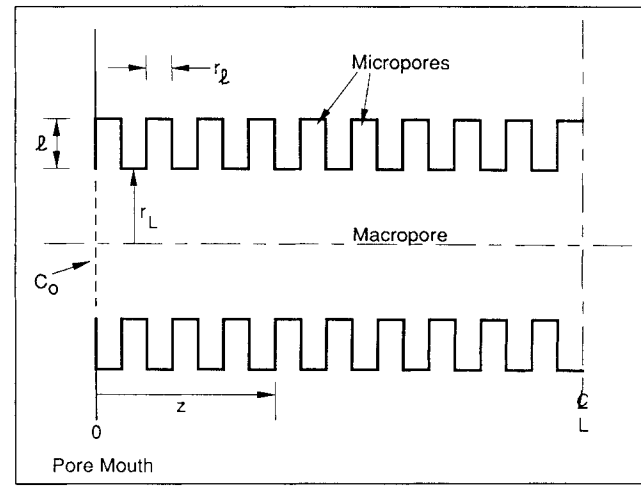

Figure 1. Bidisperse-pore system based on the Turner model.

Poisons on heterogeneous catalysts, getters in vacuum systems, and traps for poisonous gases and vapors are examples of systems that adsorb essentially irreversibly. The analytical solution and two asymptotic solutions give the adsorption-time profiles to saturation.

Theoretical Development

The bidisperse-pore system is represented on Figure 1, in which all the pores are assumed to be smooth and cylindrical. We make the usual assumptions that the dimension L is very much larger than ℓ, r_L is very much larger than r_ℓ, and r_L is of the same order of magnitude as ℓ. We assume further that the adsorbate is strongly adsorbed, essentially irreversible. A consequence of the model is that virtually all of the area on which adsorption takes place is in the micropores and that the micropores are filled with adsorbate advancing with time as a sharp front. Each micropore is divided into two regions: one completely saturated with adsorbate and the other having no adsorbate, as shown on Figure 2. A material balance of adsorbate in the micropores is given by:

$$\pi r_\ell^2 \mathcal{D}_\ell \left(\frac{C(z,t)}{y}\right) = 2\pi r_\ell \Gamma_\ell \frac{dy}{dt} \tag{1}$$

The accumulation term normally in a material balance is not present, owing to the fact that the amount of adsorbate on the surface of the micropore greatly exceeds that in the unadsorbed phase. Equation 1 is correct then when $2\pi r_\ell \Gamma_\ell \gg \pi r_\ell^2 C_o$. In Eq. 1, $C(z,t)$ is the concentration of adsorbate at the micropore mouth, $\mathcal{D}_\ell$ is the diffusivity of the adsorbate in the micropore, and Γ_ℓ is the capacity per unit area of the micropore surface for the adsorbate. Rearranging and integrating Eq. 1, we get

$$y = \left(\frac{r_\ell \mathcal{D}_\ell}{\Gamma_\ell}\right)^{1/2} \left(\int_0^t C(z,t')dt'\right)^{1/2} \tag{2}$$

or

$$\phi = \left(\int_0^\tau \psi(\zeta,\tau')d\tau'\right)^{1/2} \tag{3}$$

where

$$\psi(\zeta,\tau) \equiv \frac{C(z,t)}{C_o},\ \zeta \equiv \frac{z}{L},\ \tau \equiv \frac{t}{t_\ell},\ \phi \equiv \frac{y}{\ell}$$

and

t_ℓ = time for adsorbate at $z = 0$ to penetrate the entire micropore

From Eq. 2,

$$\ell = \left(\frac{r_\ell \mathcal{D}_\ell}{\Gamma_\ell}\right)^{1/2} (C_o t_\ell)^{1/2}$$

or

$$t_\ell = \frac{\ell^2 \Gamma_\ell}{r_\ell \mathcal{D}_\ell C_o} \tag{4}$$

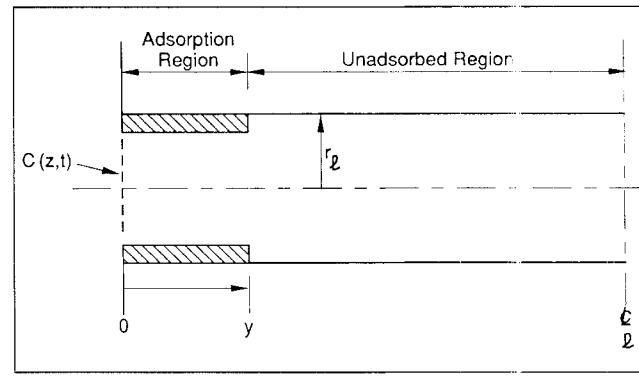

Figure 2. Micropore model.

A material balance on the adsorbate in the macropore system is

$$\pi r_L^2 \mathcal{D}_L \frac{\partial^2 C(z,t)}{\partial z^2} = \left[n\pi r_\ell^2 \mathcal{D}_\ell \frac{C(z,t)}{y}\right][2\pi r_L] + \pi r_L^2 \frac{\partial C(z,t)}{\partial t} \tag{5}$$

where n is the number of micropores per unit area of macropore surface. Again, the accumulation term, the second term on the righthand side of Eq. 5, is set equal to zero because the amount of adsorbate in the micropores greatly exceeds that in the macropore gas phase, or $4\pi r_\ell \ell n \Gamma_\ell \gg r_L C_o$.

In terms of dimensionless quantities:

$$\frac{\partial^2 \psi(\zeta,\tau)}{\partial \zeta^2} = B^2 \frac{\psi(\zeta,\tau)}{\phi} \tag{6}$$

where

$$B \equiv \left(\frac{2n\pi r_\ell^2 \mathcal{D}_\ell L^2}{\ell r_L \mathcal{D}_L}\right)^{1/2}$$

But from Eq. 3,

$$\frac{\partial \phi}{\partial \tau} = \frac{\psi(\zeta,\tau)}{\left(\int_0^\tau \psi(\zeta,\tau')d\tau'\right)^{1/2}} \tag{7}$$

Substituting Eqs. 3 and 7 into Eq. 6, we get

$$\frac{\partial^2 \psi(\zeta,\tau)}{\partial \zeta^2} = B^2 \frac{\partial \phi}{\partial \tau} \tag{8}$$

Integrating both sides of Eq. 8 with respect to τ and using Eq. 3 result in

$$\frac{d^2(\phi^2)}{d\zeta^2} = B^2 \phi \tag{9}$$

with the boundary conditions

$$\zeta = 0, \phi = \phi_0 \text{ for } 0 \le \tau \le 1$$

$$\tau = 0, \phi = 0 \text{ for all } \zeta$$

Let $\xi \equiv B\zeta$

whereupon

$$\frac{d^2(\phi^2)}{d\xi^2}=\phi \tag{10}$$

These transformations are significant because ψ is no longer in the equation explicitly and Eq. 10 is an ordinary differential equation.

Carrying out the indicated operations,

$$\frac{d^2\phi}{d\xi^2}+\frac{1}{\phi}\left(\frac{d\phi}{d\xi}\right)^2-\frac{1}{2}=0 \tag{11}$$

Now let $v\equiv(d\phi/d\xi)^2$ and substitute into Eq. 11 to obtain

$$\frac{dv}{d\phi}+\frac{2v}{\phi}-1=0 \tag{12}$$

Integrating Eq. 12 results in

$$v=\frac{\phi}{3}+\frac{\text{constant}}{\phi^2} \tag{13}$$

At this point, we seek a solution to Eq. 13 wherein ϕ goes to zero at some value of ζ in the macropore system. Accordingly, the constant in Eq. 13 must go to zero to keep v finite in the interval $0\le\zeta\le1$. A solution for the case where $\phi>0$ everywhere in the interval $0\le\zeta\le1$ is explored in Appendix B. This leads to a numerical method of solution for the amount adsorbed over a wider range of time.

Setting the constant equal to zero and substituting for v, we obtain

$$\frac{d\phi}{d\xi}=-\frac{\phi^{1/2}}{\sqrt{3}} \tag{14}$$

or

$$\phi_o^{1/2}-\phi^{1/2}=\frac{\xi}{2\sqrt{3}} \tag{15}$$

wherein we have used the boundary conditions $\phi=\phi_o$ at $\xi=0$. Substituting for ξ,

$$\phi_o^{1/2}-\phi^{1/2}=\beta\zeta \tag{16}$$

where

$$\beta\equiv\frac{B}{2\sqrt{3}}=\left(\frac{n\pi r_\ell^2\mathfrak{D}_\ell L^2}{6r_L\ell\mathfrak{D}_L}\right)^{1/2} \tag{17}$$

Equation 16 is valid provided

$$\phi=0 \text{ somewhere in } 0\le\zeta\le1 \quad \text{and} \quad \phi\le1 \tag{18}$$

In is instructive to investigate the constraints on Eq. 18. For a value of $\beta=1$, clearly $\phi_o\to1$ as $\bar{\zeta}\to1$, where $\bar{\zeta}$ is the maximum penetration in the macropore, as shown in Figure 3. In fact,

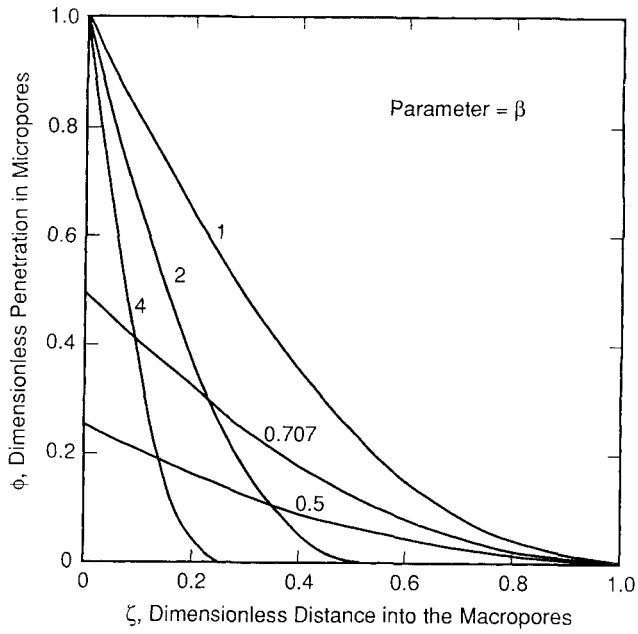

Figure 3. Micropore-macropore adsorption distribution as a function of the parameter β.

the curve corresponding to a value of $\beta=1$ represents the boundary between two regions:

$\beta>1$: a regime in which the micropores at the outside of the pellet, $z=0$, fill *before* adsorbate has penetrated to the pellet center, $z=L$

$\beta<1$: a regime in which the macropore is penetrated to the pellet center, $z=L$, before the micropores at the outside of the pellet, $z=0$, are completely filled

Time does not appear explicitly in Eq. 16; however, using Eq. 3, time is directly related to ϕ_o. That is, at the outer surface of the pellet, the concentration is constant at C_o and $\psi(\zeta,\tau)$ is equal to one. Integrating Eq. 3 gives $\tau=\phi_o^2$. Noting from Eq. 18 that ϕ_o cannot be greater than 1, it follows that Eq. 16 is valid for $\tau\le1$. In other words, Eq. 16 is valid while $\phi_o\le1$ *or* while $\bar{\zeta}\le1$, which is the meaning of Eq. 18. The penetration profiles for each region are shown on Figure 3 for various values of β at various times, each representing the longest time that Eq. 16 is valid. At longer times, we violate the conditions of Eq. 18.

The dimensionless penetration of the micropores, ϕ, decreases with increasing penetration into the macropores. According to Eq. 16, $\phi=0$ at some depth $\bar{\zeta}$:

$$\phi_o=(\beta\bar{\zeta})^2, \text{ provided } 0\le\phi_o\le1 \text{ and } 0\le\bar{\zeta}\le1. \tag{19}$$

But from Eq. 3,

$$\phi_o=\tau^{1/2} \tag{20}$$

Accordingly,

$$\bar{\zeta}\propto t^{1/4} \tag{21}$$

That is, in the range of validity of Eqs. 19 and 20 the penetration of adsorbate advances as the *fourth* root of time for

the bidispersed system, not the *square* root as is true for a monodispersed system.

Adsorption Isotherm

The adsorption uptake as a function of time is readily obtained from Eqs. 3 and 16. The total capacity of the medium for adsorbate, M_T, is:

$$M_T = (n2\pi r_\ell \ell \Gamma_\ell)(2\pi r_L L) \tag{22}$$

whereas the amount at any time, M, depends on the values of y as a function z. That is,

$$M = 4n\pi^2 r_\ell r_L \Gamma_\ell \int_0^{\bar{z}} y(z)dz \tag{23}$$

where $\bar{z} \le L$.

Combining Eqs. 22 and 23

$$F = \int_0^{\bar{\zeta}} \phi d\zeta \tag{24}$$

where $F \equiv M/M_T$, the fraction adsorbed.

From Eq. 16,

$$\phi = (\phi_o^{1/2} - \beta\xi)^2 \tag{25}$$

Substituting Eq. 25 into Eq. 24 and carrying out the integration over a range of values of $0 \le \phi \le 1$ and substituting for $\bar{\zeta} \equiv (\phi_o^{1/2})/\beta$, we get

$$F = \frac{\phi_o^{3/2}}{3\beta} \tag{26}$$

Finally, using Eqs. 20 and 26

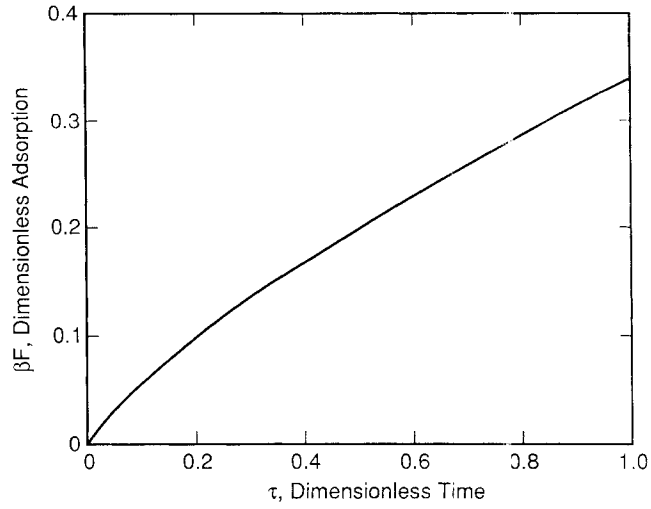

Figure 4. Fraction adsorbed vs. dimensionless time for the maximum range of validity of Eq. 16.

$$\beta F = \frac{\tau^{3/4}}{3} \tag{27}$$

Figure 4 shows this relationship up to the maximum range of validity of Eq. 16. For $\beta \ge 1$, Figure 4 is valid over the entire range of $0 \le \tau \le 1$. For values of $\beta < 1$, of course, Eq. 16 is invalid after the adsorbate has penetrated to the center of the pellet.

Thus, using Figure 4 in its range of applicability for $\beta \ge 1$, the maximum adsorption occurs when $\tau = 1$ and the corresponding value of F is $0.333/\beta$. Whereas for $\beta < 1$, the maximum τ is β^4 and at that value of τ, $F = \beta^2/3$. This range of applicability of Eq. 16 is shown in a different way on Figure 5, on which the fraction adsorbed, F, is plotted vs. τ on log-log coordinates according to Eq. 27. The lower left region displays the behavior of the analytic solution for various values of β. Note that F is small for most values of β at the boundaries of the analytical solution.

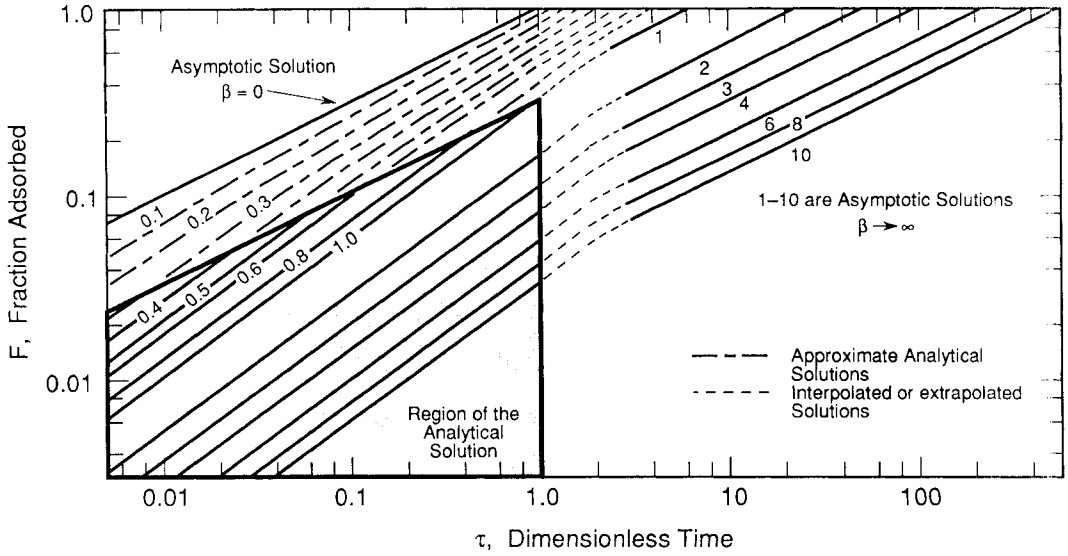

Figure 5. Fraction adsorbed vs. dimensionless time.

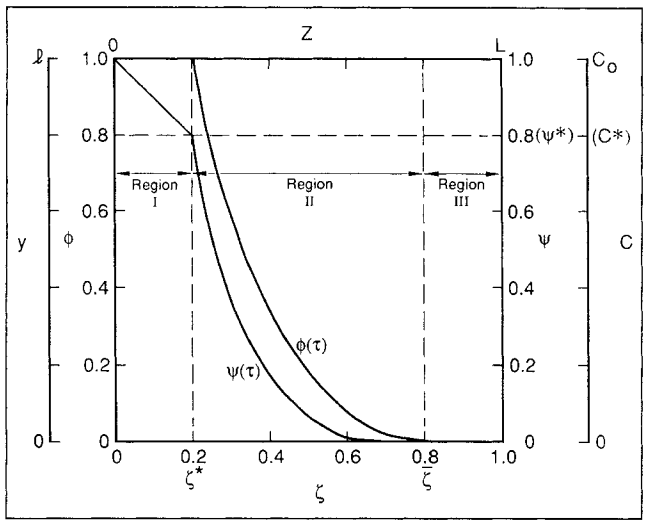

Figure 6. Auxiliary plot for the analytical solution of large values of β using a numerical method.

Extension of Solutions to High Values of Uptake

The primary purpose of this article is to explore the various behavorial regimes that are characteristic of adsorption in bidisperse pore systems and to establish criteria for that behavior in terms of the fundamental properties of the adsorbent. Equation 16 accomplishes these goals. However, at best, the analytical solution gives quantitative adsorption as a function of time up to a maximum of one third of the total adsorption. Nevertheless, it is frequently important to know the adsorption kinetics up to the capacity of the adsorbent, we discuss three methods to estimate the adsorption kinetics beyond the valid range of Eq. 16. First, we investigate the asymptotic behavior of the system of equations as β goes to zero and as β goes to infinity. Secondly, we devise a numerical method to extend the analysis to higher values of the fraction adsorbed. Third, we present an approximate analytical solution in the region where $\beta < 1$.

Let us look at the physics of the more difficult case first. When $\beta > 1$, $\bar{\zeta}$ will be less than 1 when $\phi_o = 1$ at the pore mouth. Specifically, assume $\beta = 2$. The profile for $\tau = 1$ is shown in Figure 6. The micropores at $z = 0$ are completely filled. As more adsorbate diffuses into the macropore, the adsorbate will gradually develop a region close to the external surface of the pellet wherein the micropores are entirely filled with adsorbate. Beyond this is a region where ϕ decreases from 1 at $z = z^*$ to zero at $z = \bar{z}$. This band will continue to penetrate the macropores until $\bar{z} = 1$. At $z = z^*$, the concentration of adsorbate will drop to C^* owing to the diffusion resistance of region I.

In region I, adsorbate diffuses down a tube of completely filled pores, therefore, the rate in region I in

$$\pi r_\ell^2 \mathfrak{D}_L \left(\frac{C_o - C^*(z,t)}{z^*} \right)$$

and this amount of adsorbate deposits in the pores in region II and can be represented by

$$2\pi r_L n 2\pi r_\ell \Gamma_\ell \int_{z*}^{\bar{z}} \left(\frac{\partial y}{\partial t} \right) dz$$

Equating these two expressions and making them dimensionless, we obtain in two alternate but equivalent forms:

$$\frac{1 - \psi(\zeta,\tau)}{\zeta^*} = B^2 \int_{\zeta*}^{\bar{\zeta}} \frac{\psi(\zeta,\tau)}{\phi(\zeta,\tau)} d\zeta \tag{28}$$

$$\frac{1 - \psi(\zeta,\tau)}{\zeta^*} = B^2 \int_{\zeta*}^{\bar{\zeta}} \frac{\partial \phi}{\partial \tau} d\zeta \tag{29}$$

Also from Eqs. 6 and 7:

$$\frac{\partial^2 \psi(\zeta,\tau)}{\partial \zeta^2} = B^2 \frac{\psi(\zeta,\tau)}{\phi(\zeta,\tau)} \tag{30}$$

$$\frac{\partial \phi}{\partial \tau} = \frac{\psi(\zeta,\tau)}{\phi(\zeta,\tau)} \tag{31}$$

It is clear from Figure 3 that as β becomes larger, the ϕ vs. ζ profile becomes steeper and region II gets narrower. In the limit of very large β, the boundaries of region II, ζ^* and $\bar{\zeta}$ differ by a differential amount. Simultaneously, the concentration of adsorbate falls to zero at the border between region I and region II and in essence ϕ goes from one to zero in the zone of width $d\zeta$. Equation 29 becomes

$$\frac{1}{\bar{\zeta}} = B^2 \frac{d\bar{\zeta}}{d\tau} \tag{32}$$

and leads to

$$\tau = \left(\frac{B\bar{\zeta}}{2} \right)^2 \tag{33}$$

after the boundary condition $\zeta = 0$ when $\tau = 0$ is used. Furthermore, for Eq. 24

$$F = \bar{\zeta} \tag{34}$$

and substituting Eqs. 17 and 33

$$F = \frac{\tau^{1/2}}{\sqrt{6\beta}} \tag{35}$$

Equation (35) is the asymptotic adsorption behavior for large values of β.

The corresponding asymptotic solution for small values of β obtains directly from Eq. 6, wherein B^2 is allowed to go to zero with the result

$$\frac{\partial^2 \psi}{\partial \zeta^2} \to 0. \tag{36}$$

The solution satisfying the boundary conditions, $(d\psi/d\zeta)(1,\tau) = 0$ and $\psi(0,\tau) = 1$, is $\psi(\zeta,\tau) = 1$.

All micropores are filled to the same extent. So that $\phi = \phi_o$

$$F=\phi_o \int_0^1 d\zeta$$

$$=\phi_o$$

$$=\tau^{1/2} \tag{37}$$

Equation 37 is the asymptotic solution for β going to very small values.

Equations 28–30 and 31 form the basis for a numerical extension of the analytical solution. Starting with the analytical ϕ vs. ζ solution for τ at its maximum value, one solves Eq. 30 for ψ vs. ζ by discretizing ψ and ϕ on a convenient mesh. Equation 31 can be used then to calculate $\Delta\phi$ at each mesh point to get a new ϕ profile. Repeating the procedure permits evaluation of F vs. τ. Of course, complications arise for $\beta>1$ and $\beta<1$ because the interval in ζ over which the equations are processed vary with τ. Although it is time-consuming to program, these complications offer no conceptual difficulties.

An approximate analytical solution is useful to extend the analytical solution in $\beta<1$. Obviously, Eq. 9 is still valid; however, we cannot meet the boundary condition $d\phi/d\zeta=0$ at $\zeta=1$. Nevertheless, solutions to Eq. 9 can be used to estimate the behavior outside the range of the exact solution as outlined in Appendix A.

A more exact method to extend the solution in the region when $\beta<1$ beyond the range of Eq. 16 is to use Eq. 13 for solutions where the value of ϕ does not go to zero for $0\le\zeta\le1$. This is outlined in Appendix B.

Extended Adsorption Isotherm

With the aid of the two asymptotic solutions, a few numerical solutions, and the approximate analytical solution, the remainder of Figure 5 was constructed. The ordinate is the fraction of the adsorbate capacity and the abscissa is a dimensionless time, wherein the reference time is the time required to fill a micropore at the outer surface of the pellet. In the lower left corner is a region in which the exact analytical solution is valid. All of the curves have a slope of 3/4. Above this is the asymptote for small β. The upper right part of the figure was obtained directly from Eq. 35, the large β asymptotic equation. Eventually, the slope changes from 3/4 power to the 1/2 power as τ increases, the region of changeover depending on the value of β. Dashed lines between the large β asymptotic solution and those given by Eq. 27 are sketched in to make a smooth transition. Dashed lines at low values of β have been calculated using an approximate analytical solution (see Appendix A).

Note that $\beta=0.1$ still deviates from the small β asymptotic, and the slopes of the solutions for $1\le\beta\le0.5$ vary considerably from 0.5.

Particularly interesting is the behavior of bidisperse adsorbants for the β values of the order of unity. The dimensionless time for saturation of the adsorbent varies an order of magnitude between a value of $\beta=0.7$ and $\beta=2$, the latter being larger. In this range of β values, the amount of adsorption is proportional to $\tau^{3/4}$ and, accordingly, the adsorption rate varies as $\tau^{-1/4}$ is surprisingly constant as compared to $\tau^{-1/2}$ in the regions of high adsorption and $\beta>1$. Surprising also is the narrow range between $\beta=0.2$ and $\beta=4$, where the adsorption profiles change from nearly uniform adsorption to a sharp front, as shown in Figure 3.

Zeolites represent a class of adsorbants of greatest interest to the subject of this article, since the range of values of $\mathcal{D}_\ell$ allows small values of β. Of course, ion exchange systems, wherein $\mathcal{D}_\ell$ is diffusion in a solid matrix, also offer the same possibility. In more traditional solids, such as catalysts using alumina or silica supports, the magnitude of β is so large that the rates at which irreversibly adsorbed substances accumulate within the adsorbent are limited by diffusion resistances in the macropores.

A recent study (Chmelka et al., 1990) of the adsorption of hexamethylbenzene in NaY zeolite using ^{129}Xe NMR demonstrates how the behavior of the system depends critically on the numerical magnitude of β.

$$\beta\equiv\left(\frac{n\pi r_\ell^2\mathcal{D}_\ell L^2}{6r_L\ell\mathcal{D}_L}\right)^{1/2} \tag{38}$$

where

$n\pi r_\ell^2 = \epsilon_\ell$, the porosity ≈ 0.5

$r_L \approx \ell \approx 10^{-6}$ m

$L \approx 10^{-2}$ m

$\mathcal{D}_L \approx 10^{-5}$ m^2/s

Putting these values into Eq. 38 above, we see that $\mathcal{D}_\ell$ must be of the order of 10^{-12} m^2/s for $\beta=1$. For $\mathcal{D}_\ell>10^{-12}$ will result in saturation of micropores at the mouth of the macropores before the adsorbate penetrates to the center of the pellet, whereas $\mathcal{D}_\ell<10^{-12}$ adsorbate will penetrate to the center of the pellet before the micropores at the outside of the pellet saturate. The estimated value for $\mathcal{D}_\ell$ for the aromatic adsorbate was 10^{-11} m^2/s and the adsorbate was observed experimentally to penetrate the adsorbent as a relatively sharp front. The profile for $\beta\approx\sqrt{10}$ on Figure 3 is quite sharp. Whereas, when the NaY zeolite was exposed to water vapor, the diffusivity was reduced about 2 orders of magnitude to make the $\beta\approx1/\sqrt{10}$ and the adsorbate penetrated the adsorbent almost uniformly. The corresponding adsorption profile shown on Figure 3 is quite flat. These adsorption experiments on the same zeolite under two different sets of conditions illustrate how the magnitude of β dramatically alters the nature of the adsorption process.

An estimate of the time for filling the micropores at the external surface of the pellet is given by Eq. 4.

$$t_\ell=\frac{\ell^2\Gamma_\ell}{r_\ell\mathcal{D}_\ell C_o}$$

where

$\ell = 10^{-6}$ m

$r_\ell = 10^{-9}$ m

$\mathcal{D}_\ell = 10^{-12}$ m^2/s

$\Gamma_\ell = 10^{17}$ molecules/m^2

$C_o = 10^{23}$ molecules/m^3 (i.e., partial pressure $\approx 10^{-2}$ atm)

Therefore, $t_\ell\approx1{,}000$ s. Obviously, the time for filling is inversely proportional to $\mathcal{D}_\ell$ and inversely proportional to C_o.

It is noteworthy that t_ℓ depends somewhat on geometry. As shown in Appendix C, the corresponding value for $t_{\ell,sp}$ using spherical coordinates is

$$t_{\ell,sp}=\frac{\Gamma_\ell a R_o^2}{6\epsilon_\ell\mathcal{D}_\ell C_o} \tag{39}$$

where

a = surface area per unit volume of micropore
R_o = radius of the microsphere

and all the other quantities have their previous definitions.

A simplified model of porous catalysts yields

$$\frac{a}{\epsilon_\ell} = \frac{2}{r_\ell} \tag{40}$$

Putting Eq. 40 into Eq. 39 gives:

$$t_{\ell,sp} = \frac{t_\ell}{3} \tag{41}$$

Although geometry and the form of the adsorption isotherm will change the β criterion somewhat, as defined herein it appears to be useful when compared to other systems. For example, Ruckenstein et al. (1971) used as a criterion that if

$$\frac{L^2}{\mathcal{D}_L} \geq 100 \frac{\ell^2}{\mathcal{D}_\ell},$$

then diffusion resistance in the macropores dominates. Using this criterion for the hexamethylbenzene experiments of Chmelka et al. (1990), $\mathcal{D}_\ell$ is of the order of 10^{-11} m^2/s, which is in agreement with the β criterion of this article. Because the model of Ruckenstein et al. assumes a spherical pellet, spherical microspheres, and a linear adsorption isotherm, agreement with the idealized model of this article suggests the general utility of the β criterion developed herein.

Notation

C = concentration of adsorbate in pore system
C_o = concentration of adsorbate at macropore mouth
C^* = concentration of adsorbate at z^*
F = M/M_T, fraction adsorbed
ℓ = length of micropore
L = length of macropore
M = amount adsorbed at τ
M_T = capacity of absorbent for adsorbate
n = number of micropores per unit area of macropore surface
r_ℓ = radius of micropore
r_L = radius of macropore
t = time
v = $(d\phi/d\xi)^2$, transformation variable
y = length of micropore covered with adsorbate
z = coordinate along macropore
$\bar{z}$ = penetration distance of adsorbate in macropore
z^* = distance into the macropore corresponding to completely filled micropores

Script variables

$\mathcal{D}_\ell$ = diffusivity in micropores
$\mathcal{D}_L$ = diffusivity in macropores
ξ = $B\zeta$, dimensionless distance in macropores

Greek letters

ϵ_ℓ = microporosity of adsorbant
Γ_ℓ = adsorbate capacity per unit area
ζ = z/L, dimensionless distance in macropore
$\bar{\zeta}$ = $\bar{z}/L$
ζ^* = z^*/L
ϕ = y/ℓ, fraction of a micropore that is filled
ϕ_o = y_o/ℓ, fraction of a micropore at the macropore mouth that is filled
ψ = C/C_o, dimensionless concentration

Literature Cited

Barrer, R. M., "Diffusion in Porous Media," *Appl. Math. Res.*, **2**, 129 (1963).

Chmelka, B. F., J. V. Gillis, E. E. Petersen, and C. J. Radke, "Transport of Aromatic Molecules in NaY Zeolite Powders," *AIChE J.*, **10**, 1562 (1990).

Doong, S. J., and R. T. Yang, "Bidisperse Pore Diffusion Model for Zeolite Pressure Swing Adsorption," *AIChE J.*, **33**, 1045 (1987).

Garg, D. R., and D. M. Ruthven, "The Performance of Molecular Sieve Adsorption Columns: Systems with Micropore Diffusion Control," *Chem. Eng. Sci.*, **29**, 571 (1974).

McBain, J. W., "The Adsorption of Gases and Vapours by Solids," George Routledge & Sons, London (1952).

Ruckenstein, E., A. S. Vaidyanathan, and G. R. Youngquist, "Sorption by Solids with Bidisperse Pore Structures," *Chem. Eng. Sci.*, **26**, 1305 (1971).

Turner, G. A., "The Flow Structure in Packed Beds," *Chem. Eng. Sci.*, **7**, 156 (1958).

Appendix A

In the region $\beta < 1$, Eq. 16 is valid until $\phi \to 0$ at $\zeta \to 1$, although Eq. 10 applies at times beyond the limitation of Eq. 16, the problem being that we can meet the boundary condition, $d\phi/d\zeta = 0$ at $\zeta = 1$. However, we can approximate the $\phi - \zeta$ profile for a given value of β by using the solution for a higher β, β_{ref} and by truncating it in a way that keeps the pore length constant. This is illustrated on Figure 1A. Suppose we wish to determine the $F - \zeta$ curve for $\beta = 0.5$. Up to a time $\tau = \beta^4$, F is determined from Eq. 27. At $\tau = \beta^4$, we can estimate the value of F for the case where $\phi_o = 0.525$, i.e., $\beta = 0.75$, by interpreting the curve for the solution shown on Figure 1A from $z = 0$ to $z = L$.

$$F = \frac{\int_o^L \phi dz}{\int_o^L dz} = \frac{1}{L} \int_o^L \phi dz \tag{1A}$$

Let

$$Y \equiv \frac{\phi}{\phi_o}, \quad \zeta \equiv \frac{z}{L_1}, \quad \phi_o = \beta_1^2 \tag{2A}$$

From Eq. 16,

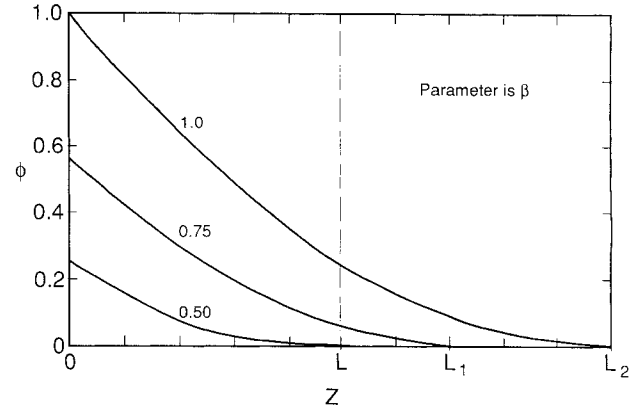

Figure 1A. Approximate solution for small values of β.

$$Y=(1-\zeta)^2 \tag{3A}$$

Substituting Eqs. 2A and 3A in Eqs. 1A

$$F=\beta_1^2\left(\frac{L_1}{L}\right)\int_o^{L/L_1} Y d\zeta \tag{4A}$$

Carrying out the integration and recognizing that $B\propto L$ and substituting accordingly for $L/L_1=\beta/\beta_1$,

$$F=\beta_1^2\left\{1-\frac{\beta}{\beta_1}+\frac{1}{3}\left(\frac{\beta}{\beta_1}\right)^2\right\} \tag{5A}$$

for $\tau=\beta_1^4$. Similarly it can be done for $\beta_1=1$.

Appendix B

When ϕ is not equal to zero in the interval of $0\le\zeta\le1$, we must evaluate the constant in Eq. 13 to meet the boundary condition that $d\phi/d\zeta=0$ when $\phi=\phi(1)$. Carrying this out and making the substitution for $\xi=2\sqrt{3}\zeta$, we get

$$\frac{1}{2\beta}\frac{\phi d\phi}{[\phi^3-\phi^3(1)]^{1/2}}=\pm d\zeta \tag{1B}$$

To integrate Eq. 1B numerically involves a singularity at $\phi=\phi(1)$ at $\zeta=1$. Accordingly, we made the substitution

$$y\equiv[\phi^3-\phi^3(1)]^{1/2} \tag{2B}$$

which resulted in

$$\frac{1}{3\beta}\int_0^{y(\phi)}\frac{dy}{[y^2-\phi^3(1)]^{1/3}}=1-\zeta \tag{3B}$$

Equation (3B) gives the ϕ vs. ζ profile as a function of $\phi(1)$ for various values of β. Equation 3B is useful particularly for determining the ϕ profiles for the case of $\beta<1$ where also $\phi_o<1$. Under these circumstances, time can be directly related to ϕ_o. The use of Eq. 3B for obtaining ϕ profiles when ϕ is equal to 1 anywhere in the micropores is valid; however, one cannot relate the profiles to time. In the latter case, time must be computed using the methods outlined in the section on Extension of Solutions to High Values of Uptake.

Appendix C

Adsorbate, which enters the microsphere through the area πR_0^2 at a rate equal to the amount of adsorbate deposited in the area $\pi\bar{R}^2\,\Gamma_\ell(d\bar{R}/dt)$, provides the following material balance equation on adsorbate.

$$\pi R_0^2\,\epsilon_i\,\mathfrak{D}_\ell\left(\frac{dC}{dR}\right)_{R=R_o}=\pi\bar{R}^2\,\Gamma_\ell\,a\,\frac{d\bar{R}}{dt} \tag{1C}$$

In the dead zone between R_o and $\bar{R}$, no adsorption takes place, so that

$$\frac{1}{R^2}\frac{d}{dR}\left(R^2\frac{dC}{dR}\right)=0 \tag{2C}$$

and

$$\left(\frac{dC}{dR}\right)_{R=R_o}=\frac{C_o}{\left(\frac{1}{R_o}-\frac{1}{\bar{R}}\right)R_o^2} \tag{3C}$$

where the boundary conditions imposed on Eq. 2C are that $C=C_o$ at R_o and $C=0$ at $R=\bar{R}$. Substituting Eq. 3C into Eq. 1C

$$\left(\frac{\epsilon_i\mathfrak{D}_\ell C_o}{\Gamma_\ell a R_0^2}\right)t=\frac{\bar{\zeta}^3}{3}-\frac{\bar{\zeta}^2}{2}+\frac{1}{6} \tag{4C}$$

where the boundary condition is used that $\bar{\zeta}=1$ at $t=0$. Thus, when $\bar{\zeta}=0$, $t=t_{\ell,sp}$

$$t_{\ell,sp}=\frac{\Gamma_\ell a R_o^2}{6\epsilon_\ell\mathfrak{D}_\ell C_o} \tag{5C}$$

A simple pore model frequency used to analyze for the average pore size is:

$$r_\ell=\frac{2\epsilon_i}{a}$$

which leads to

$$t_{\ell,sp}=\frac{R_o^2\Gamma_\ell}{3r_\ell\mathfrak{D}_\ell C_o} \tag{6C}$$

Manuscript received Nov. 19, 1990, and revision received Mar. 12, 1991.